

Vibrational Properties of CO at the Pt(111)–Solution Interface: the Anomalous Stark-Tuning Slope

V. Stamenkovic,[†] K. C. Chou,^{†,‡} G. A. Somorjai,^{†,‡} P. N. Ross,[†] and N. M. Markovic^{*,†}

Materials Science Division, Lawrence Berkeley National Laboratory, Berkeley, California 94720, and
Departments of Chemistry, University of California, Berkeley, California 94720

Received: November 12, 2004; In Final Form: December 3, 2004

Vibrational properties of CO have been studied on Pt(111) in acid and alkaline electrolytes by synchronous measurements of CO oxidation current (0.5 mV/s) and IRAS spectra (one spectrum for every 1 mV). We found that in acid solutions the frequency-tuning rate ($d\nu_{\text{CO}}/dE$) as well as the potential-dependent bandwidth ($d\Delta\nu_{1/2}/dE$) deviates from expected linear relationships. This unusual potential-dependent behavior is interpreted in terms of compression/dissipation of CO islands *during* the CO oxidation, engendered by competitive adsorption between inactive anions from a supporting electrolyte and the reactive OH species.

Introduction. The use of in situ surface sensitive probes to characterize the electrified metal–solution interfaces has yielded a wealth of structural and catalytic information. One class of electrochemical systems of particular significance, which has turned out to be suitable to characterization by vibrational spectroscopy, e.g., infrared absorption–reflection spectroscopy (IRAS) and sum frequency generation (SFG), structure sensitive probes and electrochemical (EC) methods, is carbon monoxide on Pt(111).¹ The interest in this system stems from the opportunity to relate the infrared spectral feature to the real space adlayer structures^{2,3} and in part because the anodic oxidation of CO plays a role of “test molecule” in electrocatalysis,¹ as it does in gas-phase catalysis.⁴ Although extensive EC/IRAS/SFG data have been gathered at the Pt(111)–CO interface in an electrochemical environment, the level of interpretation was limited by several factors, most importantly the temporal matching of CO vibrational properties (ν_{CO}) and the surface coverage by CO (Θ_{CO}).⁵ In our first attempt to clarify the discrepancy between the ν_{CO} vs Θ_{CO} relationship on the Pt(111) surface we used SFG spectroscopy.⁵ In these experiments we found that in the potential region where the Pt(111) surface is almost free of CO, the CO frequency exhibited an unusual blueshift deviations.⁵ The data points for the ν_{CO} vs Θ_{CO} relationship were so limited, however, that the observed deviation was questionable.

In this paper, by synchronous measurements of CO oxidation current (0.5 mV/s) and IRAS spectra (one spectrum for every 1 mV), we avoid the temporal mismatch that has troubled the interpretation of the IRAS/SFG spectra in the past. For our purposes here we fill focus only on the analysis of the anomalous potential-dependent vibrational behavior of linear and bridge CO band frequencies ($\nu_{\text{CO}}^{\text{l}}$ and $\nu_{\text{CO}}^{\text{b}}$, respectively) and corresponding O–C–O vibrational frequency of the dissolved CO₂. Although we show data for the potential-dependent vibrational behavior of multicoordinated CO, these results will not be

discussed in detail because they show well-established linear Stark-tuning relation.

Results and Discussion. Representative cyclic voltammogram of Pt(111) in 0.5 M H₂SO₄ obtained in a spectroelectrochemical cell designed for an external reflection mode in a thin layer configuration is shown in Figure 1a.

The presence of hydrogen adsorption region below 0.25 V and bisulfate/hydroxide adsorption region at higher potentials are familiar features of Pt(111) voltammetry in sulfuric acid solution. The CO-stripping curve (recorded *simultaneously* with IRAS spectra) shows that the onset of CO oxidation commences at ca. 0.35 V, forming between 0.35 < E < 0.65 V what we have previously referred to as a preignition potential region.¹ In the ignition potential region (above 0.65 V) the stripping voltammetry is characterized by a sharp peak centered at 0.68 V. In both potential regions CO oxidation takes place in the Langmuir–Hinshelwood type reaction between CO and OH ($\text{CO} + \text{OH} = \text{CO}_2 + \text{H}^+ + \text{e}^-$). In agreement with previous work², we found that on Pt(111) in CO-free acid solutions the C–O stretching bands corresponding to linear and bridge-coordinated CO predominate in the spectra. In all previous reports, the dependence of frequency ν_{CO} on the electrode potential are seen to be essentially linear, at least to potentials as high as ca. 0.45 V.^{6–9} This has been explained in two different ways, e.g., as a change in the CO chemical bonding (back-donation) with potential and as the effect of electric field on the CO molecules (the vibrational Stark effect). From a fundamental perspective, however, these are different aspects of the same phenomena.¹⁰

Figure 1b shows that the $d\nu_{\text{CO}}^{\text{l}}/dE$ and $d\nu_{\text{CO}}^{\text{b}}/dE$ dependence is, in fact, nonlinear, which to our knowledge has not been previously reported for the CO adlayer on Pt(111) in sulfuric acid solution. In particular, Figure 2b shows that a linear $d\nu_{\text{CO}}^{\text{l}}/dE$ slope (ca. 31 cm¹/V) is observed only below 0.35 V, e.g., in the potential region where CO adlayer is stable on the surface (no CO₂ production in Figure 1a). Concomitant with the development of CO₂ at 0.375 V (green curve), the $\nu_{\text{CO}}^{\text{l}}$ frequencies (red curve) first slightly increase with respect to

* Corresponding author. E-mail: nmmarkovic@lbl.gov.

[†] Lawrence Berkeley National Laboratory.

[‡] University of California, Berkeley.

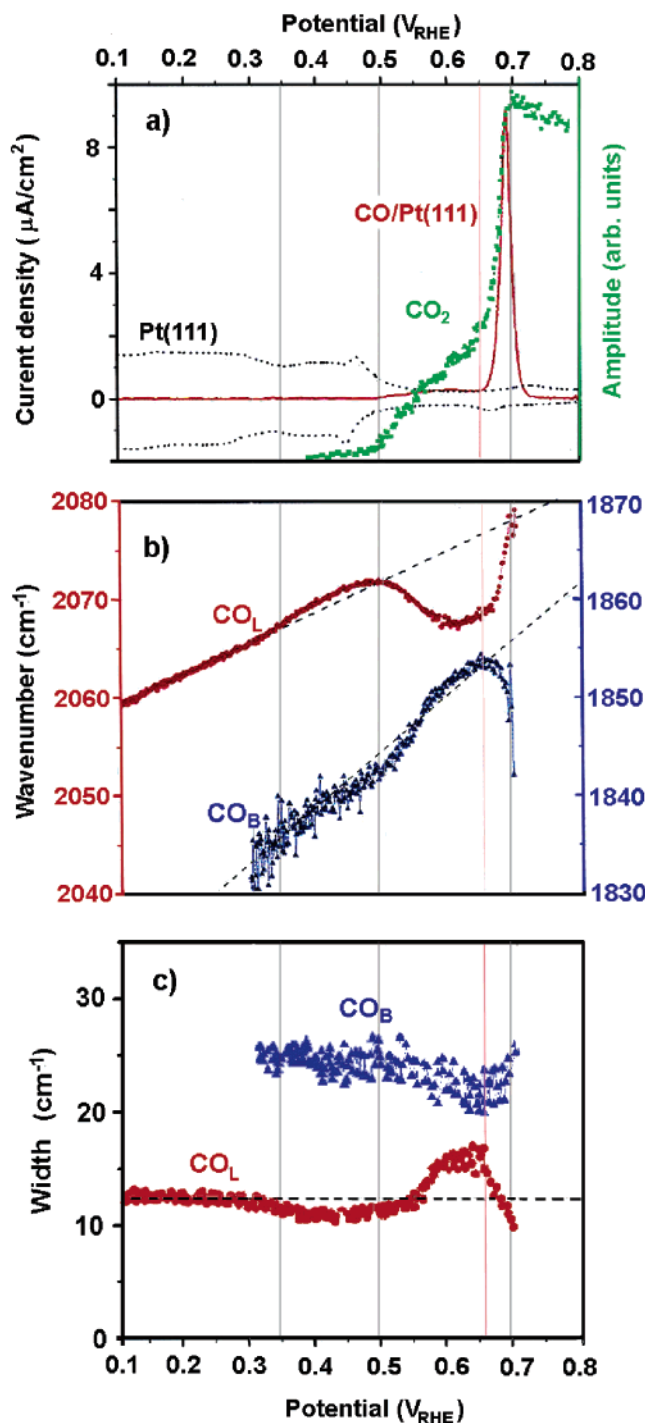


Figure 1. (a) Cyclic voltammogram of Pt(111) in 0.5 M H_2SO_4 (black trace, 2 mV/s); CO stripping current (red curve, 0.5 mV/s) and corresponding CO_2 production (green dots). (b) $d\nu_{CO}/dE$ plots recorded simultaneously with CO stripping. (c) ν_{CO} bandwidth (i.e., full width at half-maximum) vs. E .

the expected linear relation (dotted trace in Figure 1b) then, over the potential range $0.5 < E < 0.6$ V ν_{CO}^I frequencies downshift substantially with a slope of $-45\text{ cm}^{-1}/V$ and, finally, the marked increase in ν_{CO}^I frequencies above 0.65 V is mirrored by the rapid CO oxidation (CO_2 production in Figure 1a). A significant blueshift of the CO frequency at $E > 0.65$ V is unambiguous, confirming that a few SFG data points recorded previously in the same potential region were real⁵ and that the dependence of frequency ν_{CO} on the electrode potential is rather complex. Clearly, in addition to the effect of electric field, other factors, such as CO adlayer compression/dissipation should be

taken into account to explain the anomalous deviations from a linear $d\nu_{CO}^I/dE$ dependence. The phenomenon of CO adlayer compression/dissipation is observed in segregated systems where the presence of one species causes the other species to segregate into patches in which the local density is higher/lower than that observed when an equivalent amount of particular species is adsorbed alone.¹¹ Extending this phenomenon to Figure 1b, we suggest that the ν_{CO}^I frequency deviations arise from difference in both fractional coverages by the reactive (CO and OH) and inactive (HSO_4^-) intermediates and the mutual interaction among them.

The most readily explanation for ν_{CO}^I blueshift deviation between $0.35 < E < 0.5$ V is a relatively simple model, where a small yet clearly discernible CO oxidation (initiated by OH adsorption on defect sites¹²) is followed by bisulfate anion adsorption on Pt sites which below the onset of CO oxidation were occupied by CO. Given that CO- HSO_4^- interaction is most likely repulsive, higher ν_{CO}^I frequency than expected most plausibly reflects mild compression of CO islands (the enhanced dipole-dipole coupling) engendered by HSO_4^- coadsorption. On the other hand, marked ν_{CO}^I redshift observed between $0.5 < E < 0.6$ V reflects the reduced dipole-dipole coupling and temporal dissipation of CO adlayer into less compressed clusters. Such behavior is symptomatic of increased CO oxidation, induced by an enhanced OH adsorption and hindered HSO_4^- adsorption. In the potential region where intensive CO oxidation is observed ($E > 0.65$ V), however, the adsorption of bisulfate is more favorable than OH (surface provides larger ensembles of CO-free Pt sites), acting again as a driving force for CO to cluster into small compressed islands.

The formation of compressed CO islands is also confirmed from plots of the ν_{CO}^I and ν_{CO}^B bandwidth ($\Delta\nu_{1/2}$) as a function of potential. As shown in Figure 1c, while $\Delta\nu_{1/2}$ values of bridge-bonded CO stay nearly constant throughout the entire potential region, the $\Delta\nu_{1/2}$ vs. E relationship of linear bonded CO exhibits nonlinear behavior, e.g., essentially independent $\Delta\nu_{1/2}$ values ($12\text{--}13\text{ cm}^{-1}$) below $E < 0.35$ V, previously observed by Chung and Weaver for "electrooxidative stripping conditions",⁸ are followed first by the band narrowing (from 13 cm^{-1} at 0.3 V to 10 cm^{-1} at 0.55 V), then between 0.55 and 0.65 V by the band broadening (from 10 to 17.5 cm^{-1}) and, finally, above 0.65 V $\Delta\nu_{1/2}$ values again decrease from 17.5 to 9.5 cm^{-1} . Comparison of parts b and c of Figure 1 reveals marked differences in $d\nu_{CO}/dE$ and $d\Delta\nu_{1/2}/dE$ behavior; e.g., they are "oscillating in the opposite phase" along the expected linear relations, the latter being discussed in ref 8. The observation that blueshift deviations are mirrored by the band narrowing is consistent with the anion induced formation of CO islands within which CO is present at high local coverage. On the other hand, the observation that redshift deviations are accompanied by the band broadening is signaling dissipation of CO islands in the presence of excess of OH species.

To test further the anion-induced island compression model, CO oxidation experiments were carried out in CO saturated H_2SO_4 (Figure 2a), $HClO_4$ (Figure 2b) and KOH (Figure 2c) solutions. To demonstrate that the results summarized in Figure 1 are not unique to the CO stripping experiments, in Figure 2 we summarize data for the ν_{CO} vs. E relationships in CO saturated solutions.

As shown in Figure 2a, above 0.4 V in H_2SO_4 the anomalous ν_{CO}^I deviations are also observed in the presence of CO in solution. In contrast to the CO-free solution, however, due to a slow CO oxidation and continuous surface repopulation by CO, the blueshift deviations at low potentials are not clearly

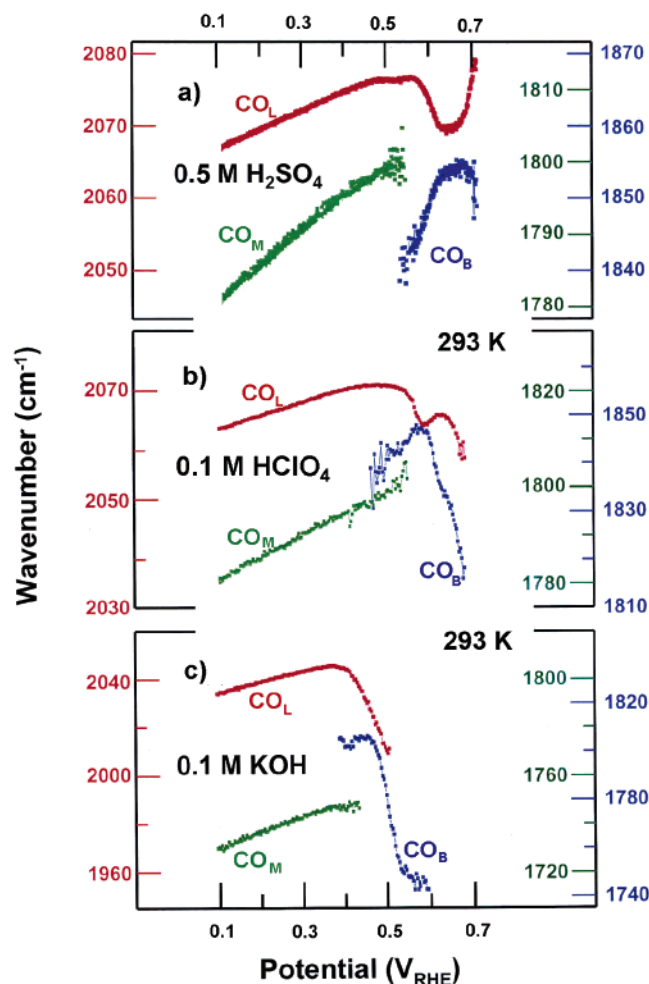


Figure 2. $d\nu_{\text{CO}}/dE$ plots for CO_{ad} in the different electrolytes. Notice the existence of multicoordinated CO in the CO saturated electrolyte; for details see refs 1 and 2.

discernible in the CO saturated solution. A comparison of representative $\nu_{\text{CO}}^{\text{I}}$ infrared spectra in the solution containing strongly (HSO_4^-) and weakly (ClO_4^-) adsorbing anions reveals that instead of an “U-shaped” the $d\nu_{\text{CO}}^{\text{I}}/dE$ dependence, characteristic for H_2SO_4 , in HClO_4 (Figure 2b) only a moderate “U-shaped” deviations are observed in the same potential range. Such behavior can be ascribed to facile CO electrooxidation in the presence of the weakly adsorbing perchloric acid anion. Therefore, in the weakly adsorbing electrolytes the $\nu_{\text{CO}}^{\text{I}}$ redshift follows from the fast oxidative removal of CO and, thus, the reduced dipole–dipole coupling. Not surprisingly, in solution containing only OH^- anions the anomalous “Stark-tuning” behavior is completely missing, so at $E > 0.4$ V only the $\nu_{\text{CO}}^{\text{I}}$ redshift deviations are observed in KOH; see Figure 2c.

In Figures 1b and 2, parts a and b, the frequency-tuning rate for bridge-bonded CO also shows nonlinearity, but in the opposite direction compared with that of linear CO. As shown in Figure 1b, the $d\nu_{\text{CO}}^{\text{b}}/dE$ dependence is linear between 0.2 and 0.3 V ($55 \text{ cm}^{-1}/\text{V}$), but above 0.3 V redshift $\nu_{\text{CO}}^{\text{b}}$ deviations from $55 \text{ cm}^{-1}/\text{V}$ are followed by blueshift deviations and finally at the most positive potential the expected negative linear slope returns. Interestingly, the $\nu_{\text{CO}}^{\text{I}}$ and $\nu_{\text{CO}}^{\text{b}}$ deviations are “oscillating in the opposite phase” along the expected linear $d\nu_{\text{CO}}/dE$ relation. The reasons why the $d\nu_{\text{CO}}^{\text{I}}/dE$ and $d\nu_{\text{CO}}^{\text{b}}/dE$ dependency deviates in the opposite direction from the expected linear slope is unclear at present. While a satisfactory understanding of such phenomena would require considerably more detailed spectral and kinetic data, the problem is clearly one that deserves further experimental and theoretical attention.

In summary, we found that both the frequency-tuning rate as well as the potential-dependent bandwidth for CO on Pt(111) in acid solutions exhibit a rather complex behavior, which has not been previously reported for the Pt(111)–CO system. For example, the $\nu_{\text{CO}}^{\text{I}}$ and $\nu_{\text{CO}}^{\text{b}}$ deviations are “oscillating in the opposite phase” along the expected linear $d\nu_{\text{CO}}/dE$ relation. Furthermore, while the blueshift deviations of $\nu_{\text{CO}}^{\text{I}}$ are mirrored by the band narrowing, the redshift deviations are accompanied by the band broadening. It has been proposed that anomalous vibrational properties of CO may arise from compression/dissipation of CO islands during the CO oxidation, engendered by competitive adsorption between inactive anions from supporting electrolyte and reactive OH.

Acknowledgment. This work was supported by the Director, Office of Science, Office of Basic Energy Sciences, Division of Materials Sciences, U.S. Department of Energy under Contract No. DE-AC03-76SF00098.

References and Notes

- (1) Markovic, N. M.; Ross, P. N. *Surf. Sci. Rep.* **2002**, *45*, 121–254 and references therein.
- (2) Villegas, I.; Weaver, M. J. *J. Chem. Phys.* **1994**, *101*, 1648.
- (3) Yoshima, K.; Song, M.; Ito, M. *Surf. Sci.* **1996**, *368*, 389.
- (4) Engel, T.; Ertl, G. *Adv. Catal.* **1979**, *28*, 1–78.
- (5) Chou, K. C.; Markovic, N. M.; Kim J.; Ross, P. N.; Somorjai, G. A. *J. Phys. Chem. B* **2003**, *107*, 1840–1844.
- (6) Kitamura, T.; Takeda, M.; Takahashi, M.; Ito, M. *Chem. Phys. Lett.* **1987**, *142*, 318.
- (7) Leung, L. W. H.; Wieckowski, A.; Weaver, M. J. *J. Phys. Chem.* **1988**, *92*, 6985–6990.
- (8) Chang, S. C.; Weaver, M. J. *J. Chem. Phys.* **1990**, *4582*–4594.
- (9) Schwegmann, S.; Tappe, W.; Korte, U. *Surf. Sci.* **1995**, *334*, 55–76.
- (10) Lambert, D. K. *Electrochim. Acta* **1995**, *41*, 623–630 and references therein.
- (11) White, J. M.; Akhter, S. *Crit. Rev. Solid State Mater. Sci.*; CRC: 1988; pp 131–173.
- (12) Markovic, N. M.; Schmidt, T. J.; Grgur, B. N.; Gasteiger, H. A.; Ross Jr., P. N.; Behm, R. J. *J. Phys. Chem. B* **1999**, *103*, 8568–8577.